Flow simulation of fiber reinforced self compacting concrete using Lattice Boltzmann method

[1]Oldřich Švec[1]*
[1] *Technical University of Denmark, Department of Civil Engineering, Lyngby, Denmark*
[2]Jan Skoček
[2] *Technical University of Denmark, Department of Civil Engineering, Lyngby, Denmark*
[3]Henrik Stang, [3]John Forbes Olesen; [3]Peter Noe Poulsen
[3] *Technical University of Denmark, Department of Civil Engineering, Lyngby, Denmark*

Abstract
Self compacting concrete (SCC) is a promising material in the civil engineering industry. One of the benefits of the SCC is a fast and simplified casting followed by decreased labor costs. The SCC as any other type of concrete has a significantly lower tensile and shear strength in comparison to the compression strength and, therefore, it needs to be reinforced. Fiber reinforced concrete is an alternative to traditional stirrups reinforcement leading to lowered labor costs. To be able to access mechanical properties of the fiber reinforced concrete, knowledge of final spread and directions of fibers is necessary. Computational fluid dynamics (CFD) comes to play at this stage. Formulation of a possible CFD model that is able to solve multi-phase and multi component non-Newtonian flow with complex boundary conditions and fiber suspension and preferably in reasonable time brings a very challenging task.
A relatively new group of models - Lattice Boltzmann Modeling (LBM) - is presented in this paper. The conventional LBM is modified to include fiber and particle suspensions and non-Newtonian rheology and is used to model the fiber reinforced self compacting concrete flow.

Originality
Application of Lattice Boltzmann Modeling to the field of fiber reinforced self compacting concrete is a novelty. It is the first paper dealing with multiphase flow with fiber shaped particle suspension and non-Newtonian rheology.

Chief contributions
One of the main contributions presented by the paper is the ability to predict final dispersion and orientation of fibers in the fiber reinforced self compacting concrete and thus to allocate possible problematic places. Such a prediction is not possible in other conventional methods in a comparable computational time.

Keywords: *Steel fiber reinforced concrete, Lattice Boltzmann method, Immersed Boundary method*

[1] Corresponding author: Email olsv@byg.dtu.dk Tel +45 4525 1940

1 INTRODUCTION

In the past, one of the main bottlenecks in application of steel fiber reinforced concrete for load carrying structures has been the lack of design rules and design tools including the absence of safety factors taking into account knowledge of expected variations in material properties and structural performance. It is believed that fiber orientation and distribution plays an important role in the final properties of structural elements and it is thus desirable to understand the underlying phenomena governing the final fiber distribution and orientation. Extensive experimental work becomes relatively expensive and time consuming and therefore simulations capable describing the nature of the problem might be an appropriate alternative.

In this paper a relatively new Lattice Boltzmann Method (LBM) (Aidun & Clausen, 2010) is being used as a Computational Fluid Dynamics (CFD) solver to simulate a non-Newtonian flow of the self compacting concrete (SCC). Particles of any shape such as round or elongated are implemented in the form of a force field using a modified Immersed Boundary Method (IBM) with direct forcing (Feng & Michaelides, 2005). A new non-linear dynamics algorithm has been developed and is being applied to ensure stability of the simulation (Skocek et al., 2011). Free surface is implemented using a mass tracking algorithm (Körner et al., 2005).

2 LATTICE BOLTZMANN

In the traditional CFD tools such as the Finite Volume Method, the problem is formulated in the form of macroscopic quantities, namely spatially and time dependent velocity and pressure fields. The LBM on the other hand, with its roots in the kinetic theory of gases, treats fluid as particle distributions where the particles can be seen as e.g. molecules. Discrete particle distribution functions are used to discretize the particle distributions. The LBM provides rules for mutual collisions and propagation of the particle distributions as well as for the computation of the macroscopic quantities.

In the framework of the LBM, space is usually discretized by a set of Eulerian cells of a uniform size. Similarly, time is discretized into uniform time steps. Usually, the space and time spacing, as well as a reference density of the fluid are set to unity and the real problem is scaled accordingly. Dimensionless lattice units are considered if not stated otherwise. Each Eulerian cell has one lattice node in its center. The lattice node holds a set of N discrete particle distributions $f_\alpha, \alpha = 1...N$ for different lattice velocities.

The LBM equation can then be written as

$$f_\alpha(\mathbf{x}+\mathbf{c}_\alpha\Delta t, t+\Delta t) = f_\alpha(\mathbf{x},t) + \Omega_\alpha(\mathbf{x},t), \tag{1}$$

where $\mathbf{c}_\alpha$ is a microscopic lattice velocity of the particle distribution and $\Omega_\alpha(\mathbf{x},t)$ is a collision operator. The lattice velocities are in the order of the speed of sound i.e. in the order of 1. The LBM for an incompressible fluid is valid only for low Mach numbers and therefore $\mathbf{u}_f(\mathbf{x}) \ll 1$, where $\mathbf{u}_f$ is a macroscopic velocity of the fluid. Local density can be computed as a sum of particle distributions in one node

$$\rho(\mathbf{x},t) = \sum_{\alpha=1}^{N} f_\alpha(\mathbf{x},t) \tag{2}$$

and local velocity as a sum of particle distributions in one node multiplied by their respective lattice velocities $\mathbf{c}_\alpha$

$$\mathbf{u}_f(\mathbf{x},t) = \frac{1}{\rho(\mathbf{x},t)} \sum_{\alpha=1}^{N} f_\alpha(\mathbf{x},t)\mathbf{c}_\alpha. \tag{3}$$

The equations presented above comprise almost all ingredients required for the fully working LBM. Some parts such as the collision operator $\Omega_\alpha(\mathbf{x},t)$ were omitted for brevity. The LBM therefore has a

relatively simple implementation and reasoning for the given problem. The code is also easily parallelized since most of the parts of the LBM core require local information only.

Further information regarding the LBM may be obtained from (Sukop & Thorne, 2005; Wolf-Gladrow, 2000).

3 IMMERSED BOUNDARY METHOD MODIFICATION

The Immersed Boundary Method (IBM) will in short be introduced via an stationary example of a single solid body immersed in a flow as presented in Figure 1. In the framework of the IBM, the fluid observes the body in the form of a force field. Traditionally one would measure momentum exchange caused by particle distributions hitting the body for a unit time. In the IBM, the particle distributions are allowed to penetrate the solid body. At the end of each time step the penetrated particle distributions are measured and corresponding forces F are exerted both back on the fluid and on the body. The total force exerted on the body is defined as

$$F = \int_V \rho_f(\mathbf{x})(\mathbf{u}_f(\mathbf{x}) - \mathbf{u}_b(\mathbf{x}))dV, \tag{4}$$

where $\rho_f(\mathbf{x})$, $\mathbf{u}_f(\mathbf{x})$ and $\mathbf{u}_b(\mathbf{x})$ stand for the local density of the fluid, local velocity of the fluid and local velocity of the immersed body. V is the volume of the body.

Measuring the amount of particle distributions penetrating the solid body is a crucial part and, as will be shown, it restricts the usage of the IBM to bodies of the minimum size larger than $\sqrt{2}$ lattice units. Outer particle distributions are schematically shown in Figure 1 A as hollow dots. Inner particle distributions are not displayed for simplicity. All the particle distributions can be measured macroscopically by a local velocity as presented in Eq. (3).

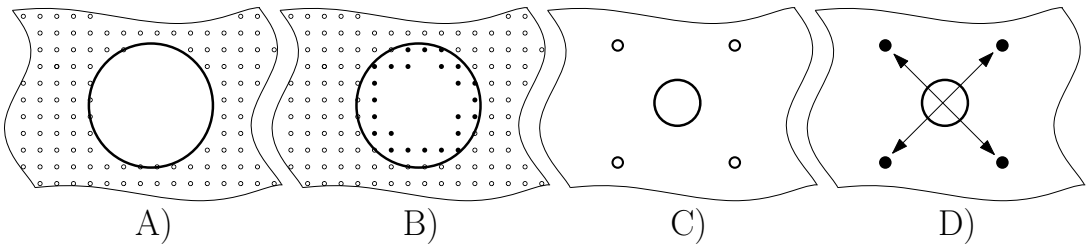

Figure 1: Representation of particle distributions penetrating a solid body

Having $\mathbf{u}_f(\mathbf{x}_b) = \mathbf{0}$, where $\mathbf{x}_b \in V$, suggests, that no outer particle distributions penetrated the stationary solid body in that region. Contrary to this, a non-zero velocity $\mathbf{u}_f(\mathbf{x}_b) \neq \mathbf{0}$ suggests that particle distributions originating outside of the body have reached the region inside the body and therefore should be accounted for by the immersed boundary force. This is schematically shown in Figure 1 B, where filled dots are outer particle distributions that penetrated the body in the previous time step. Decreasing the minimum size of the body, outer particle distributions penetrating the solid body will stream through the whole body and leave the body on the other side during one time step as presented in Figure 1 C, D. Thus, the local velocity field no longer describes penetrating particle distributions correctly. The more particle distributions leave the body, i.e. the smaller the body is with respect to spatial discretization, the higher inaccuracy is observed as shown in Figure 3. Therefore, the minimum size of the element is equal to the speed of particle distributions and is in the range of $\sqrt{2}$ lattice units.

Fibers are bodies with traditionally high aspect ratio. For the case of steel fibers the aspect ratio ranges between 30 - 80. The discretized length of the fiber would have to be 40 - 110 lattice units to satisfy the above mentioned condition. This would significantly restrict the usage of the method and hence a correction of the method is explored in the following.

3.1 *Fitting the Correction term*

Drag force on an infinite circular cylinder midway between two parallel plates has been measured using an uncorrected version of the IBM and compared to an empirical solution as described in (Benrichou, 2004). Geometry of the problem is shown in Figure 2. The flow is driven by a Poiseuille velocity profile

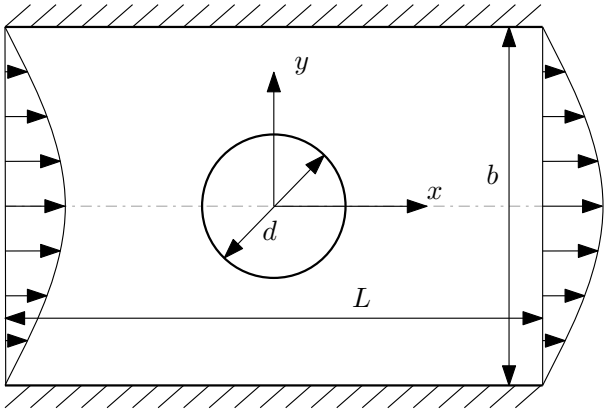

Figure 2: Geometry of the Poiseuille flow model

placed both at the inflow and at the outflow. An empirical drag force is computed as

$$F_x = \mu U_{x,max} \frac{\pi(4k^2 - 8)}{1.9362 - 3.7520k^2 + 2\ln(k)} \tag{5}$$

where F_x is the drag force, $U_{x,max}$ is the maximum speed of the defined Poiseuille flow and $k = d/b$ is the fraction of the cylinder diameter and the channel width. The empirical solution in Eq. (5) is valid only for a Newtonian flow at very low Reynolds numbers and for $k < 0.4$. In all the simulations, the Reynolds number has been set to 0.1. The length of the channel has been set to value of $L = \max(30d, 30)$, the width of the channel to $b = 20$ and the diameter of the cylinder ranges from 0.3 up to 5 lattice units. A Newton - Raphson method has been used for each of the diameters to find a correction term C, such as to equalize the simulation drag force F with the empirical one F_x, assuming

$$F_x = F = C \int_{\Omega} \rho_f(\mathbf{x})(\mathbf{u}_f(\mathbf{x}) - \mathbf{u}_p(\mathbf{x}))dV. \tag{6}$$

It has been found out that the correction term can be approximated by

$$C = \begin{cases} 1.8d^{-1.2}, & d < 1.5 \quad (7) \\ 1, & d > 1.5. \quad (8) \end{cases}$$

Figure 3 presents an error of the drag force as a function of the cylinder diameter both for a corrected and uncorrected version of the IBM. It is clearly seen, that such a simple fitting function significantly reduces the error from 80 % to 3 % for the diameter 0.3.

The Couette flow test has been run to support the suggested correction term.

4 COUETTE FLOW

A suspension of steel fibers of various volume fractions immersed in a Bingham fluid were subjected to the Couette flow. The geometry of the problem can be seen in Figure 4. The following values were

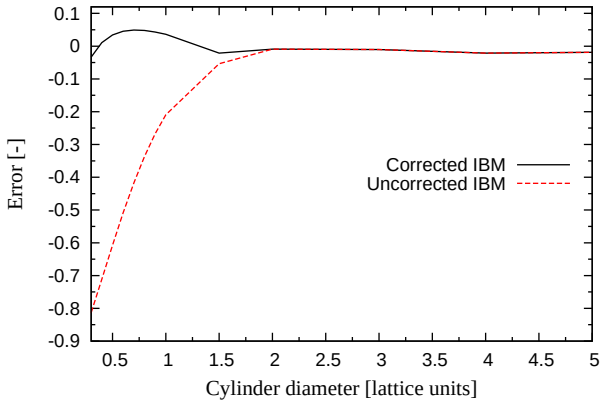

Figure 3: Error of the IBM simulation before and after correction

considered: $L_p = 0.06$ m corresponding to 12 lattice units, aspect ratio of the fiber 37.5, $L_x = L_z = 2L_p$, $L_y = 4L_p$, $\rho_p = 7000$ kgm^{-3}, $\rho_f = 2160$ kgm^{-3}, $\tau_y = 5$ Pa and $\mu_{pl} = 10$ Pas. The simulation was performed for three shear rates equal to 0.4 s^{-1}, 4.0 s^{-1} and 10.0 s^{-1} respectively, and for volume fractions ranging between 0.001 and 0.04.

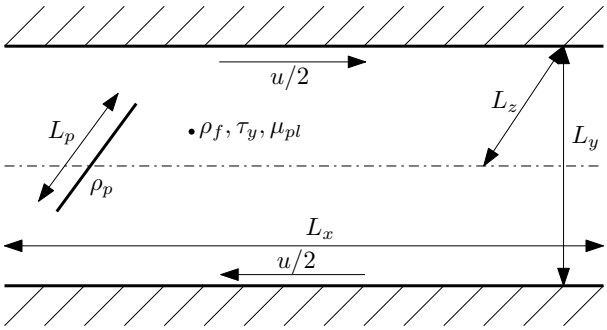

Figure 4: Couette flow geometry.

Resulting effective viscosities μ_{eff} were computed from the stresses acting on the boundary walls. Shear rates were obtained by a volume averaging of the fluid between the walls excluding zones closer than $0.5L_p$ to walls. An assumption that the resulting effective fluid is a Bingham fluid has been applied.

Figure 5 shows a relation of the relative viscosity μ_{eff}/μ_{pl} for different volume concentrations of fibers. The computed values are compared with a relation by (Ghanbari & Karihaloo, 2009) both for the case of the corrected and uncorrected version of the IBM represented as filled and hollow marks respectively. A simulation of fibers with no rotation allowed has been run (circular marks) together with simulations of fibers with allowed rotation (square and triangular marks). Simulations of fibers with allowed rotations were further divided into two simulations, one with lubrication forces deactivated (square marks) (Yamane et al., 1994) and the other with lubrication forces activated (triangular marks).

Looking at hollow and filled marks, one can observe that the IBM correction term apparently helps to catch correctly the underlying physics and therefore results in more realistic values of the dynamic viscosity comparable to (Ghanbari & Karihaloo, 2009). The IBM correction plays an important role even for fibers with allowed rotation as shown by square and triangular marks. Increase of the viscosity due to lubrication forces can be observed in the figure comparing square and triangular hollow marks. The lubrication forces, however, play a less significant role in comparison to the IBM correction term for the investigated volume fractions.

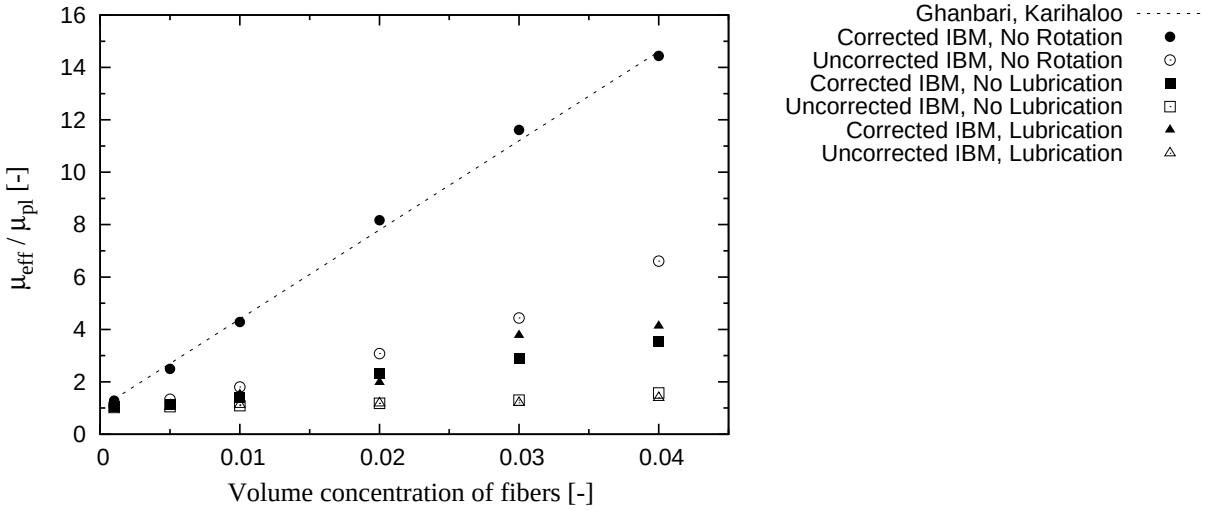

Figure 5: Relative viscosity comparison for different volume concentrations of fibers

5 SLUMP TEST

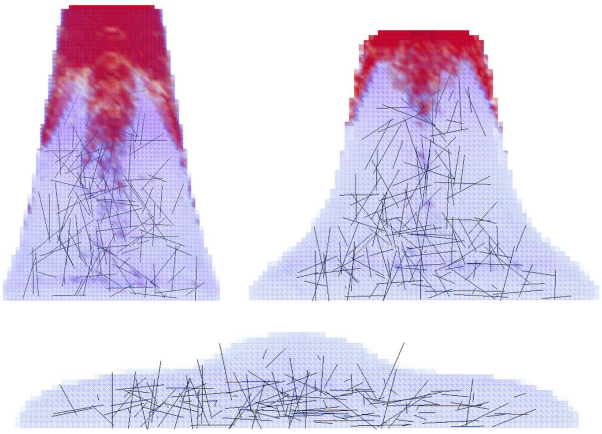

Figure 6: Slump test time snaps. Color stands for viscosity.

The slump test has been modeled to present the capabilities of the method. A Cone of height 0.3 m, base radius 0.1 m and top radius 0.05 m has been filled with the Bingham fluid of dynamic plastic viscosity 10 Pas and yield stress 5 Pa. Steel fibers of the length = 0.05 m, aspect ratio = 37.5 and fiber volume fraction = 0.2 % have been used in the simulation. Length of fibers corresponds to 12.5 lattice units and diameter to 0.33 lattice units. A correction term from Eq. (7) has been applied. The shape of the cone and distribution of fibers at 3 different time snaps are shown in Figure 6.

As for the efficiency of the code, it takes ca. 30 minutes using Intel Core 2 Due E8400 CPU with 3 GB of RAM to run 0.1 second of the simulation corresponding to 407 time steps. The fibers would have to be at minimum 54 lattice units long without the correction term to obtain correct immersed boundary forces. 0.1 second of the simulation would then take $\approx 1400\times$ longer i.e. 1 month and the memory consumption would also grow significantly.

6 CONCLUSIONS

The Lattice Boltzmann method together with the corrected Immersed boundary method and mass tracking algorithm has been applied to simulate a non-Newtonian liquid together with a particle inclusion. A correction term of the IBM has been proposed and determined by fitting, to allow for particles of a minimum size less than $\sqrt{2}$ to be included in the modeling. Fibers of a diameter not less than 0.3 lattice units have been used so far and some of the results such as Couette flow or Slump test are presented in this paper.

The presented model is based on well established methods and provides an efficient tool that can be applied to a range of engineering problems on different length scales yielding results matching favorably theoretical or experimental findings in a reasonable amount of time and using a reasonable amount computation power.

7 ACKNOWLEDGMENTS

Support from the Innovation Consortium: "Sustainable Concrete Structures with Steel Fibres - The SFRC Consortium" funded by the Danish Agency for Science Technology and Innovation is acknowledged.

References

C. K. Aidun & J. R. Clausen (2010). 'Lattice-Boltzmann Method for Complex Flows'. *Annual Review of Fluid Mechanics* **42**(1):439–472.

A. Benrichou (2004). 'Drag force on a circular cylinder midway between two parallel plates at very low Reynolds numbers - Part 1: Poiseuille flow (numerical)'. *Chemical Engineering Science* **59**(15):3215–3222.

Z. Feng & E. Michaelides (2005). 'Proteus: a direct forcing method in the simulations of particulate flows'. *Journal of Computational Physics* **202**(1):20–51.

A. Ghanbari & B. L. Karihaloo (2009). 'Prediction of the plastic viscosity of self-compacting steel fibre reinforced concrete'. *Cement and Concrete Research* **39**(12):1209–1216.

C. Körner, et al. (2005). 'Lattice Boltzmann Model for Free Surface Flow for Modeling Foaming'. *Journal of Statistical Physics* **121**(1-2):179–196.

J. Skocek, et al. (2011). 'Modeling of flow of flow of particles in non-Newtonian fluid using lattice Boltzmann method'. In *Proceedings of ICCC*.

M. C. Sukop & D. T. Thorne (2005). *Lattice Boltzmann Modeling: An Introduction for Geoscientists and Engineers*. Springer.

D. A. Wolf-Gladrow (2000). *Lattice-Gas Cellular Automata and Lattice Boltzmann Models: An Introduction (Lecture Notes in Mathematics)*. Springer.

Y. Yamane, et al. (1994). 'Numerical simulation of semi-dilute suspensions of rodlike particles in shear flow'. *Journal of Non-Newtonian Fluid Mechanics* **54**:405–421.